

DYNAMIC TEMPERATURE EFFECTS IN A CLEARANCE-SEALED PISTON PROVER FOR GAS FLOW MEASUREMENTS

J. Kutin, G. Bobovnik and I. Bajsić

Laboratory of Measurements in Process Engineering, Faculty of Mechanical Engineering,
University of Ljubljana, Aškerčeva 6, SI-1000 Ljubljana, Slovenia

E: joze.kutin@fs.uni-lj.si

This paper deals with the dynamic temperature effects in a high-speed, clearance-sealed realization of a piston prover. A dynamic mathematical model was built to study the temperature variations and to estimate their influence on the flow measurements. The mathematical model is formulated on the basis of lumped-element models of the piston and the gas cavity. The energy balance for the gas cavity includes the convective heat exchange with the surroundings. One of the potential effects results from the temperature differences between the inlet gas flow and the cylinder wall. In addition, the piston prover's operation generates dynamic temperature variations, which are mainly related to the pressure change due to the flow redirection and to the pressure oscillations due to the piston's resonance effects.

Introduction

The piston-prover concept is widely used for primary standards in the field of gas flow measurements [1–7]. The general principle of operation is based on determining the time interval that a piston needs to pass a known volume of gas at a defined pressure and temperature.

The simulation cases presented in this paper are focused on a commercially available, high-speed, clearance-sealed realization of the piston prover [8, 9]. This instrument originally employs the so-called isothermal measurement model, which can be written as for the mass flow rate:

$$q_m^{(T)} = \rho(p_a, T_{in}) \left(\frac{V_m}{\Delta t} + q_{v,l} \right) \left[\frac{p_2}{p_a} + \frac{(p_2 - p_1) V_d}{p_a V_m} \right], \quad (1)$$

where $\rho(p_a, T_{in})$ is the gas density at the barometric pressure p_a and the time-averaged inlet temperature T_{in} , V_m is the measuring volume of the gas collected by the piston prover during the timing cycle Δt , $q_{v,l}$ is the Poiseuille clearance leakage flow (the Couette leakage flow component is considered as a reduced value of V_m), p_1 and p_2 are the absolute gas pressures at the start and at the end of the timing cycle, respectively, and V_d is the volume of gas at the start of the timing cycle. The isothermal assumption of the measurement model (1) was found to be incomplete for capturing the effects of relatively high-frequency oscillations of the gas, which occur in the piston prover under discussion and have a quasi-adiabatic nature. In [10, 11] the authors of this paper derived and validated the so-called adiabatic measurement model, which can be written as:

$$q_m^{(A)} = \rho(p_a, T_{in}) \left(\frac{V_m}{\Delta t} + q_{v,l} \right) \cdot \left[\frac{p_m}{p_a} + \frac{(p_2 - p_m)}{\gamma p_a} + \frac{(p_2 - p_1) V_d}{\gamma p_a V_m} \right], \quad (2)$$

where p_m is the time-averaged value of the absolute gas pressure during the timing cycle and γ is the adiabatic index.

Neither of the measurement models (1) and (2) account for the heat exchange between the gas and the surroundings during the piston prover's operation. The aim of this paper is to estimate the potential influences of such effects. Thus, a mathematical model of the piston prover, which includes the effects of the convective heat exchange, is employed. The main properties of the model are presented in this paper, but see, for instance, [12–14] for details of the derivation of similar lumped-element models.

Mathematical model

The geometrical parameters of the mathematical model are schematically presented in Figure 1. The main modelling assumptions are as follows:

- The piston with the weight mg is modelled as a solid body with one degree of freedom that is defined by its position x in an upward direction along the cylinder.
- The damping force on the piston is modelled as a nonlinear function of the piston velocity v , that is $cv + kv|v|$, where c and k represent the damping coefficients. The damping force takes into account the clearance-fluid viscous friction and the outflow pressure losses down to atmospheric pressure p_a .
- The gas in the cavity with volume $V = Ax$, $A = \pi D^2/4$, below the piston is assumed to be ideal. Besides the ideal gas law, the following relations are valid: $\gamma = c_p/c_v$ and $c_p = c_v + R$, where γ is the adiabatic index, c_p is the specific heat at constant pressure, c_v is the specific heat at constant volume and R is the gas constant.
- The pressure p in the gas cavity is considered to be spatially homogeneous, which holds true for the wavelengths of the pressure oscillations, which are large compared with the linear dimensions of the cavity.
- The inlet flow into the gas cavity is steady with the mass flow rate q_m and the temperature T_{in} . Its

enthalpy flow rate is considered in the energy equation for the gas cavity, but the potential and kinetic energy terms are neglected. The leakage flow through the piston-cylinder clearance is neglected.

- The energy equation includes the heat exchange with the surroundings, which is modelled as the convective heat transfer between the gas cavity with the spatially averaged temperature T and the cylinder wall with the temperature T_w . The convective heat transfer coefficient is α_w and the surface area is $A_w = \pi Dx$.

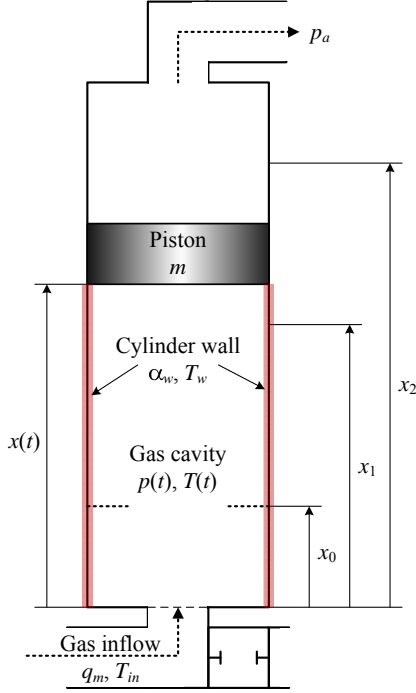


Figure 1. Model of the piston prover

Considering the force balance for the piston and both the energy balance and the ideal gas law for the gas cavity, the mathematical model can be written as a system of four, nonlinear, first-order differential equations for the piston position $x(t)$, the piston velocity $v(t)$, the gas-cavity pressure $p(t)$ and the gas-cavity temperature $T(t)$ as a function of time t :

$$\dot{x} = v,$$

$$\dot{v} = \frac{1}{m}[(p - p_a)A - mg - cv - kv|v|],$$

$$\dot{p} = \frac{1}{Ax}[\gamma q_m RT_{in} - \gamma pAv - (\gamma - 1)\alpha_w \pi Dx(T - T_w)], \quad (3)$$

$$\dot{T} = \frac{T}{pAx}[q_m R(\gamma T_{in} - T) - (\gamma - 1)pAv - (\gamma - 1)\alpha_w \pi Dx(T - T_w)].$$

The system of differential equations was solved in Mathcad (Mathsoft, Ver. 12.1) using the fourth-order, Runge-Kutta, fixed-step method ("rkfixed" built-in function), for the initial conditions $x(0) = x_0$, $v(0) = 0$, $p(0) = p_a$ and $T(0) = T_{in}$, with 10^5 constant time-steps within the piston stroke between x_0 and $1.01x_2$.

The simulations were performed for the following input data: $D = 0.0445$ m, $\Delta x = x_2 - x_1 = 0.0762$ m, $x_1/\Delta x = 1.8$, $x_0/\Delta x = 0.6$, $m = 0.021$ kg, $g = 9.806$ ms⁻², $c = 1$ Nms⁻¹, $k = 1.8$ Nm²s⁻², $R = 287$ Jkg⁻¹K⁻¹, $\gamma = 1.4$, $p_a = 98$ kPa, $T_w = 295.15$ K, $\alpha_w = (0 \dots 20; 200)$ Wm⁻²K⁻¹, $T_{in} - T_w = (0 \dots 1)$ K and $q_m = (25 \dots 50)$ g/min. The chosen input data correspond approximately to the properties of the piston prover Cal=Trak SL-800-44 (Sierra Instruments) carrying out the air flow measurements, which was already studied by the authors of this paper in [10, 11]. The piston mass and the damping coefficients were estimated by approximating the measurement results for the time-averaged gas pressure [11] with the steady-state solution of the mathematical model without the heat-exchange effects:

$$p_0 - p_a = \frac{mg}{A} + \frac{c}{A}v_0 + \frac{k}{A}v_0^2, \quad v_0 = \frac{q_m RT_{in}}{p_0 A}, \quad (4)$$

which is presented in Figure 2.

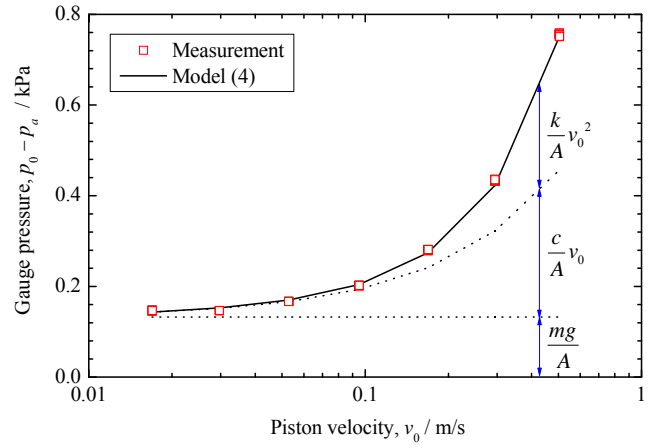


Figure 2. Approximation of the measurement results for the time-averaged gauge pressure

Results

Figure 3 shows an example of the pressure and the temperature response in the gas cavity during the piston prover's operation, calculated for $q_m = 25$ g/min, $T_{in} = T_w + 0.6$ K and two different convective heat transfer coefficients. A redirection of the gas flow into the measuring cylinder of the piston prover causes the initial transient pressure response, which reaches its steady-state value in approximately 0.15 s. The temperature is subjected to a comparable transient response, but it also varies afterwards. Because the gas with the temperature T_{in} flows constantly in the gas cavity, the initial increase in the average temperature slowly diminishes, in spite of the adiabatic conditions ($\alpha_w = 0$ Wm⁻²K⁻¹). If the heat exchange with the colder cylinder wall is considered ($\alpha_w = 10$ Wm⁻²K⁻¹), the subsequent temperature variations are still more intensified. However, the presented case does not show a noticeable heat-transfer effect on the pressure response during the timing cycle.

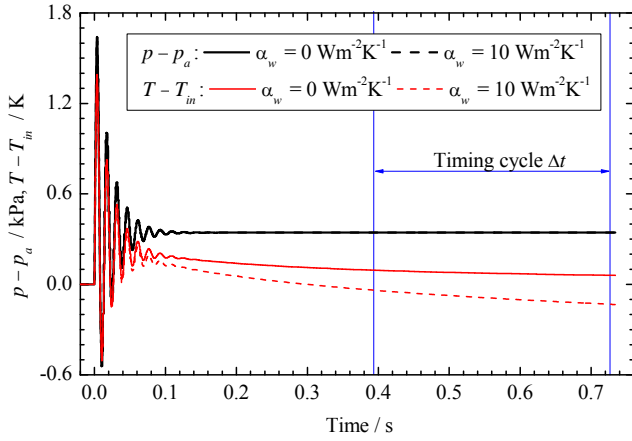


Figure 3. Time variation of the pressure and the temperature for two different convective heat transfer coefficients ($q_m = 25$ g/min, $T_{in} = T_w + 0.6$ K)

The measurement models of the piston prover presented in Section 1 result from the energy-balance equation of the gas cavity, which does not consider the heat exchange with the surroundings. The resulting relative errors of the estimated flow rate are presented in Figure 4. Simulations were performed for two different inlet flow rates of $q_m = 25$ g/min and $q_m = 50$ g/min, for different temperature differences $T_{in} - T_w$ and for different convective heat transfer coefficients α_w . The presented results are identical for both the isothermal and the adiabatic measurement model.

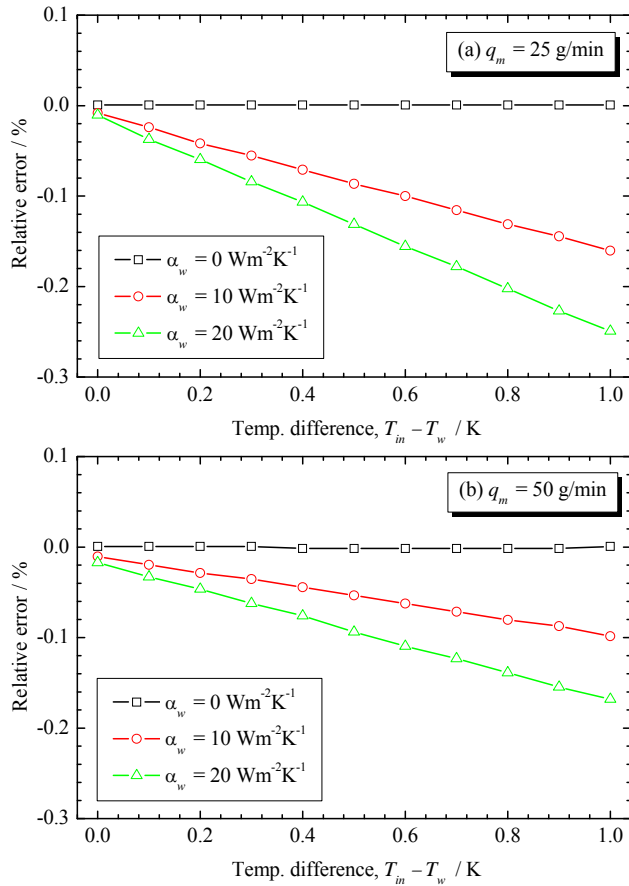


Figure 4. Relative error of the flow rate estimated by the isothermal and the adiabatic measurement model (identical results for both models)

The flow errors increase with the values of $T_{in} - T_w$ and α_w , but they are larger at the smaller flow rate. The flow errors of a few hundredths of a percent, which are evident for $T_{in} = T_w$, are related to the initial change of the average temperature due to the pressure response.

In practice the temperature differences $T_{in} - T_w$ may arise not only from the “external” temperature differences between the medium and the surroundings, but also from the flow dissipation effects, the internal heating effects of the piston prover’s electronics, etc. It is to be expected that the temperature differences between the gas and the cylinder wall are at least partially reduced after several consecutive measurement cycles of the piston prover due to the warming of the cylinder.

A key question for applying the presented simulation results to the actual instrument is a reasonable value of the effective convective heat transfer coefficient. Under the developing laminar flow conditions in the cylindrical tube, the relation $\alpha_w \propto q_m^{1/3}$ is expected [15]; α_w is estimated to be about 10 $\text{Wm}^{-2}\text{K}^{-1}$ for the largest flow rate in the case under discussion. However, the complex flow conditions in the actual realization of the piston prover (with the jet/wake inlet flow, the moving piston boundary, the coupled resonance effects [10]) make it difficult to give a more accurate estimate of α_w without further numerical or experimental studies.

The next simulations illustrate the effects of oscillating conditions in the gas cavity during the timing cycle. Like in [10], the excitation is introduced through the sinusoidal time variation of the viscous damping coefficient c , which may result from a rocking motion of the piston. For instance, c is assumed to be replaced with $c [1 + 0.2 \sin(2\pi 36t + \phi)]$, where the initial phase ϕ is randomly chosen from the interval $[-\pi, \pi]$ for each simulation case. The random initial phase is considered to illustrate the range of dispersion of the estimated flow rates, but we should bear in mind that the periodic excitations can be rather deterministic in the actual piston prover [11].

Figure 5 shows an example of the resulting pressure and temperature responses. If not properly taken into account, the oscillating temperatures at the start and at the end of the timing cycle lead to additional errors in the estimated flow rates. As is evident from Figure 6, the adiabatic measurement model, in contrast to the isothermal measurement model, efficiently determines the flow rate under such oscillating conditions, and this is also when considering the heat exchange with $\alpha_w = 20$ $\text{Wm}^{-2}\text{K}^{-1}$.

The validity of the adiabatic assumption is expected as long as the dynamic processes in the gas are fast with respect to the heat exchange. The thermal time constant [12] may be used as a measure of the thermal responsiveness of the gas cavity:

$$\tau = \frac{\rho V c_v}{\alpha_w A_w} \approx \frac{p_a D c_v}{4 R T_w \alpha_w} \quad (5)$$

Considering $\alpha_w = 20$ $\text{Wm}^{-2}\text{K}^{-1}$ and $c_v = 718$ $\text{Jkg}^{-1}\text{K}^{-1}$, the time constant is $\tau = 0.46$ s, which is about 17-times larger

than the 1/36 s time period of the oscillations. By way of illustration, we performed another simulation with a 10-times larger value of the convective heat transfer coefficient ($\alpha_w = 200 \text{ Wm}^{-2}\text{K}^{-1}$; thus $\tau = 0.046 \text{ s}$); although the experimental standard deviation of the flow rate estimated by the adiabatic measurement model shows an increase in the dispersion, it is still about 16-times smaller than in the case of the isothermal measurement model (this ratio is about 57 for the simulation results presented in Figure 6 for $\alpha_w = 20 \text{ Wm}^{-2}\text{K}^{-1}$).

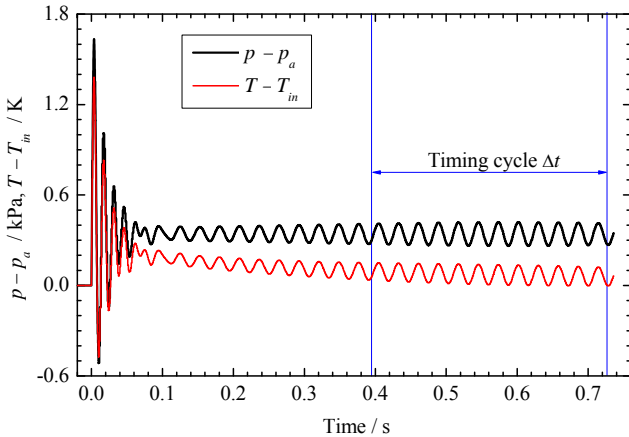


Figure 5. Time variation of the pressure and the temperature considering the periodic damping effects ($q_m = 25 \text{ g/min}$, $T_{in} = T_w$, $\alpha_w = 0 \text{ Wm}^{-2}\text{K}^{-1}$)

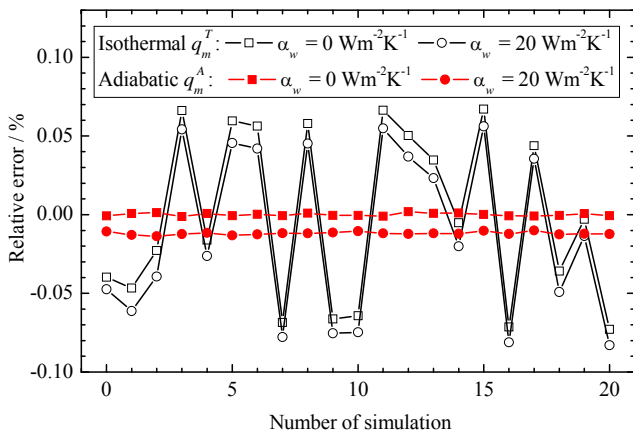


Figure 6. Relative error of the flow rate estimated by the isothermal and the adiabatic measurement models ($q_m = 25 \text{ g/min}$, $T_{in} = T_w$)

Conclusions

The purpose of this paper was to present the dynamic temperature effects in a high-speed, clearance-sealed realization of the piston prover. The analysis was performed using the dynamic, lumped-element mathematical model, which includes the effects of the convective heat exchange with the surroundings. The errors of the estimated flow rate by the piston prover were studied for the isothermal and the adiabatic measurement models, which both take into account the dynamic gas pressures at the start and at the end of the

timing cycle, but the gas temperature is considered as the time-averaged value of the inlet flow.

The heat exchange with the surroundings affects the thermodynamic processes in the gas, which are slow with respect to the heat exchange. The simulations show such processes in the observed system in connection with the initial change of the average pressure or the temperature differences of the inlet flow. The temperature variations during the timing cycle, which result from the heat exchange, may cause flow errors for the isothermal or the adiabatic measurement model.

In contrast, the oscillating thermodynamic processes in the gas that result from the piston's resonance effects are found fast with respect to the heat exchange in the observed system. Whereas the adiabatic measurement model efficiently compensates the effects of the corresponding oscillating temperatures, they may result in additional flow errors when using the isothermal measurement model.

References

- [1] J.D. Wright and G.E. Mattingly, NIST Calibration Services for Gas Flow Meters – Piston Prover and Bell Prover Gas Flow Facilities, Gaithersburg, MD: National Institute of Standards and Technology, 1998.
- [2] J.D. Wright, G.E. Mattingly, S. Nakao, Y. Yokoi and M. Takamoto, "International comparison of a NIST primary standard with an NRLM transfer standard for small mass flow rates of nitrogen gas", Metrologia, Vol. 35, pp. 211–221, 1998.
- [3] R.F. Berg and G. Cignolo, "NIST–IMGC comparison of gas flows below one litre per minute", Metrologia, Vol. 40, pp. 154–158, 2003.
- [4] G. Cignolo, F. Alasia, A. Capelli, R. Gorla and G. La Piana, "A primary standard piston prover for measurement of very small gas flows: an update", Sensor Review, Vol. 25, pp. 40–45, 2005.
- [5] S. Sillanpää, B. Niederhauser and M. Heinonen, "Comparison of the primary low gas flow standards between MIKES and METAS", Measurement, Vol. 39, pp. 26–33, 2006.
- [6] H.M. Choi, K.-A. Park, Y.K. Oh and Y.M. Choi, "Improvement and uncertainty evaluation of mercury sealed piston prover using laser interferometer", Flow Measurement and Instrumentation, Vol. 20, pp. 200–205, 2009.
- [7] C.-M. Su, W.-T. Lin and S. Masri, "Establishment and verification of a primary low-pressure gas flow standard at NIMT", MAPAN – Journal of Metrology Society of India, Vol. 26, pp. 173–186, 2011.

- [8] H. Padden, "Uncertainty analysis of a high-speed dry piston flow prover", in Measurement Science Conference (Anaheim, CA), 2002.
- [9] H. Padden, "Development of a 0.2% high-speed dry piston prover", in Measurement Science Conference (Anaheim, CA), 2003.
- [10] J. Kutin, G. Bobovnik and I. Bajsić, "Dynamic effects in a clearance-sealed piston prover for gas flow measurements", Metrologia, Vol. 48, pp. 123–132, 2011.
- [11] J. Kutin, G. Bobovnik and I. Bajsić, "Dynamic pressure corrections in a clearance-sealed piston prover for gas flow measurements", Metrologia, Vol. 50, pp. 66–72, 2013.
- [12] M. Sorli, L. Gastaldi, E. Codina and S. Heras, "Dynamic analysis of pneumatic actuators", Simulation Practice and Theory, Vol. 7, pp. 589–602, 1999.
- [13] J.F. Carneiro and F.G. Almeida, "Reduced-order thermodynamic models for servo-pneumatic actuator chambers", Proc. IMechE, Part I: Journal of Systems and Control Engineering, Vol. 220, pp. 301–314, 2006.
- [14] D. Dihovicni and N. Nedić, "Simulation, animation and program support for a high performance pneumatic force actuator system", Mathematical and Computer Modelling, Vol. 48, pp. 761–768, 2008.
- [15] J.R. Welty, C.E. Wicks, R.E. Wilson and G.L. Rorrer, Fundamentals of Momentum, Heat, and Mass Transfer, Hoboken, NJ: John Wiley & Sons, 2008.